

GLOBAL MODAL ANALYSIS OF DISK GALAXIES: APPLICATION TO AN S0 GALAXY NGC 3115

TATSUO UEDA,¹ MASAFUMI NOGUCHI,² MASANORI IYE,^{2,3} AND SHINKO AOKI²

Received 1983 December 8; accepted 1984 July 12

ABSTRACT

The global modal analysis of oscillations is applied to a series of models for NGC 3115. All the models in this series are consistent with the observed rotation curve and the observed velocity dispersion curve of NGC 3115 but have different halo mass fractions. The apparent lack of any spiral structure in this galaxy implies that the disk is stable, and this requirement gives a loose lower limit for the halo mass fraction of 30% of the total mass. This estimate is independent of photometric evaluation, and the result, although modest, is consistent with the photometric estimate.

Subject headings: galaxies: individual — galaxies: internal motions — galaxies: structure

I. INTRODUCTION

Hunter (1963, 1965) introduced a powerful scheme for studying the global oscillations of self-gravitating disk models of galaxies. This scheme makes use of a global expansion of perturbations in terms of the associated Legendre polynomials and reduces the problem of oscillations to an eigenvalue problem. Since this method is global, in contrast to the local density wave theory (cf. Lin and Shu 1964), it is appropriate for the study of the origin of lower order spatial eigenmodes, e.g., bar and/or global spiral structures.

Hunter's formulation, which was applicable only to cold disks with finite radius, has been extended by Bardeen (1975), Takahara (1976, 1978), Iye (1978), and Aoki, Noguchi, and Iye (1979, hereafter ANI) in order to deal with more general models, including warm disks, disks with static halos, and disks with an infinite radius. A similar approach using Bessel functions instead of Legendre functions was introduced by Yabushita (1969) and extended recently by Ambastha and Varma (1982, 1983).

All of these analyses, however, dealt with theoreticians' mathematical models, which sometimes fail to be realistic. No attempt was made to study the oscillations of a realistic model of any disk galaxies based on observed data because the velocity dispersion data were not available, except at the very center of some galaxies, until very recently. Owing to the development of observing technique, however, an increasing amount of data on velocity dispersion curves is becoming available mainly for early-type galaxies (cf. Illingworth 1981).

We have chosen NGC 3115 as the first galaxy to be studied by means of the global modal analysis in this paper, because this is the first galaxy whose velocity dispersion curve in the disk has been obtained, although it is not sure so far that this is the best example for studying the dynamical approach used here. NGC 3115 is a field S0[−] galaxy seen almost edge-on from us, and has been observed intensively both kinematically and photometrically. Rubin, Peterson, and Ford (1980) derived a rotation curve along the major axis of this galaxy. Illingworth and Schechter (1982, hereafter IS) presented the rotation velocity profiles and the velocity dispersion profiles along a

number of slits placed on and off the major and minor axes. The rotation velocity $V(r)$ and the velocity dispersion $\sigma(r)$ along the major axis observed by these authors are plotted in Figure 1.

Knowing the three-dimensional field of centrifugal force and the pressure gradient, one can in principle obtain the gravitational force field to balance these, and hence calculate the appropriate distribution of mass to produce such a gravitational field. We, however, cannot hope to make use of such *perfect* data at present. The scheme becomes complicated without some constraints in models of galaxies. In this paper, we make use only of kinematical data along the major axis and assume a disk-halo composite model. A series of equilibrium models with a varying halo-mass fraction is constructed to be consistent with $V(r)$ and $\sigma(r)$ of NGC 3115. The details of this scheme are described in § II.

On the other hand, the photometric studies of NGC 3115 were given by Strom *et al.* (1977), Tsikoudi (1979), and Hamabe (1982). Slight humps are seen in the luminosity profile along the major axis, and there is the possibility of the existence of rings or "relic" spiral arms (Strom *et al.* 1977; Tsikoudi 1979).

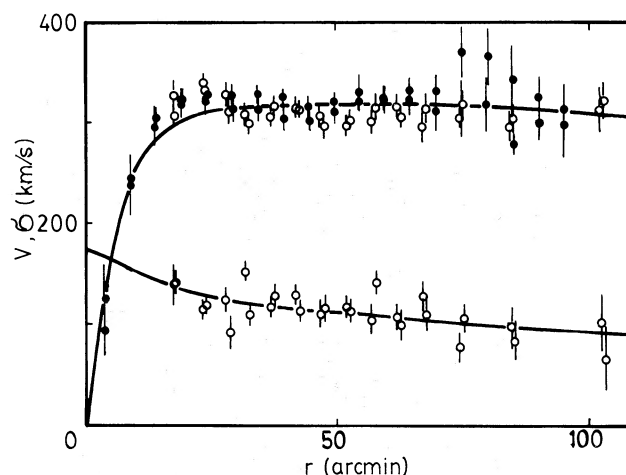


FIG. 1.—The rotation curve and the velocity dispersion curve of the models (solid lines) are compared with the observational data. The filled circles are the data given by Rubin, Peterson, and Ford (1980), and open circles are the data of IS. Considering the effect of integration along the line of sight, the values of rotation velocity are multiplied by a factor 1.2, following IS.

¹ Department of Astronomy, University of Tokyo.

² Tokyo Astronomical Observatory, University of Tokyo.

³ European Southern Observatory.

The major features are, however, smooth and symmetric. No apparent dust lane, which often associates with spiral or bar structures, can be seen. Although no one can tell the face-on appearance of this galaxy, it is unlikely that NGC 3115 has conspicuous non-axisymmetric structure. We interpret the smoothness and lack of any conspicuous feature to indicate that this galaxy is in a dynamically stable equilibrium. This is, admittedly, a working hypothesis on which we rely throughout this paper, and should not be regarded as an obvious fact.

Combining this stability requirement implied from morphology to the global stability analysis of the series of models constructed for NGC 3115, we can find the lower limit of the halo mass. The procedure of analysis is described in § III, and the results are given and discussed in § IV.

II. MODELS OF NGC 3115

We construct a sequence of models that are axisymmetric and in dynamical equilibrium. Every model is consistent with the observed $V(r)$ and $\sigma(r)$. The models are assumed to consist of two components: an infinitesimally thin disk and a spherical halo. The mass fraction of the halo component, which cannot be determined directly from the observed data, is the only parameter of this sequence of models. The structure of the two components is described hydrodynamically instead of by using a detailed distribution function of the stars comprising each component. The halo component is assumed not to rotate.

a) A Model without a Halo

To start with, we consider an extreme case where a model consists only of a disk component without a halo. Kuz'min (1956) and Toomre (1963) introduced a family of infinitesimally thin disk models for which both the surface density distribution $\mu(r)$ and its gravitational potential $\psi(r)$ on the disk plane can be expressed in simple analytical functions. Superposing a number of these disks, one can construct reasonable disk models. We restrict ourselves, for simplicity, to composite disks made up of Toomre's Model 1 disks with various masses and scale lengths. Inclusion of "Model n " disks may be straightforward but is not justified by the additional complication. We assume

$$\mu(r) = \sum_{i=1}^N \mu_i(r) = \sum_{i=1}^N \frac{M_i}{2\pi a_i^2} \left(1 + \frac{r^2}{a_i^2}\right)^{-3/2}, \quad (2.1)$$

$$\psi(r) = \sum_{i=1}^N \psi_i(r) = - \sum_{i=1}^N \frac{GM_i}{a_i} \left(1 + \frac{r^2}{a_i^2}\right)^{-1/2}, \quad (2.2)$$

where M_i and a_i are the mass and the scale length of the i th disk subcomponent, respectively. Note that for Toomre's Model 1 disks there is a simple relation,

$$\psi_i(r) = c_i [\mu_i(r)]^{1/3}, \quad (2.3)$$

where $c_i = -(2\pi)^{1/3} GM_i^{2/3} / a_i^{2/3}$. Space density $\rho(r, z)$ and gravitational potential $\psi(r, z)$ in cylindrical coordinates are related to $\mu(r)$ and $\psi(r)$ as $\rho(r, z) = \mu(r)\delta(z)$, and $\psi(r) = \psi(r, 0)$, respectively.

The random motion of stars within the plane of the disk is described by a two-dimensional pressure $P(r)$, which is assumed to be barotropic, so that we can write the enthalpy $\varphi(r)$ in an integrable form:

$$\varphi(r) = \int \frac{dP(r)}{\mu(r)}. \quad (2.4)$$

In the present paper, we assume, for greater simplicity, a specific polytropic pressure,

$$P(r) = K[\mu(r)]^\Gamma, \quad (2.5)$$

where Γ is a two-dimensional polytropic index and K is a constant. From equations (2.4) and (2.5), it follows that

$$\varphi(r) = \frac{K\Gamma}{\Gamma-1} [\mu(r)]^{\Gamma-1}. \quad (2.6)$$

The velocity dispersion $\sigma(r)$ can be expressed by

$$\sigma^2(r) = \frac{P(r)}{\mu(r)} = K[\mu(r)]^{\Gamma-1}. \quad (2.7)$$

Equation (2.7) means that the isotropic velocity dispersion is assumed. A theoretical approach taking into consideration the anisotropic dispersion is reported by one of the present authors elsewhere (Aoki 1984). The velocity dispersion $\sigma(r)$ used here is considered as an intermediate value between σ_{RR} and $\sigma_{\theta\theta}$.

The rotation velocity $V(r)$ in dynamical balance is given by

$$V^2(r) = r \frac{d\Psi(r)}{dr}, \quad (2.8)$$

where the effective potential $\Psi(r)$ is the sum of gravitational potential $\psi(r)$ and enthalpy $\varphi(r)$ of the composite disk:

$$\Psi(r) = \psi(r) + \varphi(r). \quad (2.9)$$

Equations (2.3) and (2.6) show that $\psi(r)$ and $\varphi(r)$ share the same r -dependence for a single disk model ($N = 1$) when Γ is 4/3. We use this polytropic index throughout the following discussion.

The gravitational potential energy W , internal thermal energy U , and rotational energy T of the disk are defined by

$$W = \frac{1}{2} \int_0^\infty \psi(r) \mu(r) 2\pi r dr, \quad (2.10a)$$

$$U = \int_0^\infty P(r) 2\pi r dr, \quad (2.10b)$$

$$T = \int_0^\infty \frac{1}{2} \mu(r) V^2(r) 2\pi r dr. \quad (2.10c)$$

The ratio ϵ of energy in random motion of stars to the total kinematic energy is a convenient dimensionless indicator of the disk temperature, and it can be written as

$$\epsilon = \frac{U}{|W + U + T|} = \frac{2U}{|W|} = \frac{W + 2T}{W}, \quad (2.11)$$

where the virial theorem is used to derive the second and third equations.

After some trials to fit the observed $V(r)$ and $\sigma(r)$ of NGC 3115, we found that three disk subcomponents ($N = 3$) are necessary and sufficient to reproduce the curves within the observational error allowance. The best-fit disk model of NGC 3115 has the following parameters:

$$a_1 = 0.45 \text{ kpc}, \quad a_2 = 0.90 \text{ kpc}, \quad a_3 = 3.60 \text{ kpc},$$

$$M_1 = 2.15 \times 10^{10} M_\odot, \quad M_2 = 2.15 \times 10^{10} M_\odot,$$

$$M_3 = 17.2 \times 10^{10} M_\odot, \quad \epsilon = 0.20.$$

We assume that the distance to this galaxy is 9.5 Mpc, which is derived with $H_0 = 50 \text{ km s}^{-1} \text{ Mpc}^{-1}$. Figure 1 shows $V(r)$ and $\sigma(r)$ of this model as well as the observed data for NGC 3115.

b) *Models with a Halo*

It is possible to alter the disk model of NGC 3115 constructed in the previous subsection to include a halo component without changing $V(r)$ and $\sigma(r)$ of the disk component. This can be achieved by using the fact that the gravitational potential of Toomre's Model 1 disk has the r -dependence in the plane of the disk identical with that of Plummer's (1911) spherical model.

We now consider a composite disk-halo model with its gravitational potential $\psi(r, z)$ and density $\rho(r, z)$ defined by

$$\psi(r, z) = \psi_d(r, z) + \psi_h(r, z), \quad (2.12)$$

$$\rho(r, z) = \mu_d(r)\delta(z) + \rho_h(r, z), \quad (2.13)$$

and

$$\mu_d(r) = (1-s) \sum_{i=1}^3 \frac{M_i}{2\pi a_i^2} \left(1 + \frac{r^2}{a_i^2}\right)^{-3/2}, \quad (2.14)$$

$$\rho_h(r, z) = s \sum_{i=1}^3 \frac{3M_i}{4\pi a_i^3} \left(1 + \frac{r^2 + z^2}{a_i^2}\right)^{-5/2}, \quad (2.15)$$

$$\psi_d(r, z) = -(1-s) \sum_{i=1}^3 \frac{GM_i}{a_i} \left[\frac{(a_i + |z|)^2 + r^2}{a_i^2} \right]^{-1/2}, \quad (2.16)$$

$$\psi_h(r, z) = -s \sum_{i=1}^3 \frac{GM_i}{a_i} \left(\frac{a_i^2 + z^2 + r^2}{a_i^2} \right)^{-1/2}, \quad (2.17)$$

where s is the fraction of mass of the halo component, and subscripts d and h denote the disk and halo components, respectively. We assume, for simplicity, a common scale length between the i th pair of disk and halo subcomponents.

The two-dimensional pressure of the disk is assumed again to be a $\Gamma = 4/3$ polytrope; thus

$$P_d(r) = K_d[\mu_d(r)]^{4/3}. \quad (2.18)$$

The enthalpy of the disk is here

$$\varphi_d(r, 0) = 4K_d[\mu_d(r)]^{1/3}. \quad (2.19)$$

The velocity dispersion of the disk is given by

$$\begin{aligned} \sigma_d^2(r) &= \frac{P_d(r)}{\mu_d(r)} \\ &= K_d(1-s)^{1/3} \left[\sum_{i=1}^3 \left(\frac{M_i}{2\pi a_i^2} \right) \left(1 + \frac{r^2}{a_i^2} \right)^{-3/2} \right]^{1/3}. \end{aligned} \quad (2.20)$$

We can choose the value of K_d as

$$K_d(s) = K_d(0)(1-s)^{-1/3}, \quad (2.21)$$

where $K_d(0)$ means the constant K in the haloless model, so that the velocity dispersion $\sigma_d(r)$ remains unchanged even if we shift the fraction s of the mass from disk to halo. The relation (2.21) also makes the effective potential in the plane, $\Psi(r, 0)$, independent of s :

$$\begin{aligned} \Psi(r, 0) &= \psi(r, 0) + \varphi(r, 0) \\ &= - \sum_{i=1}^3 \frac{GM_i}{a_i} \left(1 + \frac{r^2}{a_i^2} \right)^{-1/2} \\ &\quad + 4K_d(0) \left[\sum_{i=1}^3 \left(\frac{M_i}{2\pi a_i^2} \right) \left(1 + \frac{r^2}{a_i^2} \right)^{-3/2} \right]^{1/3}. \end{aligned} \quad (2.22)$$

Therefore, the rotational velocity of the disk, $V_d(r)$, remains the

same as that obtained for the haloless model in the previous subsection, and it is given by

$$V_d^2(r) = V^2(r) = r \frac{d}{dr} \Psi(r, 0). \quad (2.23)$$

The halo component can also be in dynamical equilibrium. One can derive the pressure distribution of the halo component $p_h(r, z)$ necessary to support it from the following equation:

$$\frac{1}{\rho_h(r, z)} \nabla p_h(r, z) = -\nabla \psi(r, z). \quad (2.24)$$

Since the contribution of ψ_d makes the equipotential surfaces of ψ different from spheres, this halo pressure is not generally barotropic except when $s = 1$. In order to study the stability of the disk component itself, one can, however, avoid solving the complicated partial differential equation (2.24). Equations (2.10) can be generalized for these composite models as

$$W = \frac{1}{2} \int_{-\infty}^{\infty} \int_0^{\infty} (\psi_d + \psi_h) [\mu_d \delta(z) + \rho_h] 2\pi r dr dz, \quad (2.25a)$$

$$U = \int_{-\infty}^{\infty} \int_0^{\infty} [P_d \delta(z) + p_h] 2\pi r dr dz, \quad (2.25b)$$

$$T = \int_0^{\infty} \frac{1}{2} \mu_d V_d^2 2\pi r dr. \quad (2.25c)$$

The dimensionless temperature ϵ of composite models, which are consistent with the observed $V(r)$ and $\sigma(r)$, is an increasing function of s along the model sequence. For the haloless model ($s = 0$), $\epsilon = 0.2$, and for the other extreme of diskless model ($s = 1$), $\epsilon = 1.0$, because the model is entirely pressure-supported.

We have thus constructed a sequence of equilibrium models. They all have the same rotation curve and velocity dispersion curve, which are consistent with the observed data of NGC 3115. A free parameter s , the fraction of the halo mass in the total mass, specifies a model in this sequence.

III. MODAL ANALYSIS

We study the dynamical stability of the models of NGC 3115 constructed in § II. The larger part of the analysis follows the formulation and the notations of ANI. Only the necessary modifications of ANI are described in this section and in the Appendix.

Each model has two components, but only the global stability of the disk is studied. Although the gravitational effect of the halo component in equilibrium is fully taken into account, the halo component itself is not perturbed. This is justified because the pressure-supported halo is dynamically stable. The perturbed quantities are, therefore, μ'_d , ψ'_d , φ'_d , u'_d , and v'_d of the disk component. These variables should follow the linearized Poisson equation, linearized equations of continuity and of motion, and equation of polytropic perturbation.

We adopt a normalization of variables as in equation (4.16) of ANI, but specifying their M and a to be the total mass $M = \sum_{i=1}^3 M_i = 2.15 \times 10^{11} M_\odot$ of the model and the scale length $a = 1.80$ kpc:

$$\begin{aligned} \hat{\omega} &= \left(\frac{GM}{a^3} \right)^{-1/2} \omega, & \hat{\Omega} &= \left(\frac{GM}{a^3} \right)^{-1/2} \frac{V}{r}, \\ \hat{\kappa}^2 &= \left(\frac{GM}{a^3} \right)^{-1/2} \left(\frac{V}{r} + \frac{dV}{dr} \right), & \hat{\mu}_d &= \left(\frac{M}{2\pi a^2} \right)^{-1} \mu_d. \end{aligned} \quad (3.1)$$

This gives the time unit, $(GM/a^3)^{-1/2} = 2.46 \times 10^6$ years. Note that among the quantities in equations (3.1) only $\hat{\mu}_d$ is dependent on s and proportional to $1 - s$.

With these modifications, we arrive at an eigenvalue problem of a real-valued matrix, of the form

$$\begin{pmatrix} A & B & C \\ D & A & F \\ G & H & A \end{pmatrix} \begin{pmatrix} \mathbf{a} \\ \mathbf{b} \\ \mathbf{c} \end{pmatrix} = \hat{\omega} \begin{pmatrix} \mathbf{a} \\ \mathbf{b} \\ \mathbf{c} \end{pmatrix}. \quad (3.2)$$

In equation (3.2), just as in equation (5.3) of ANI, A, B, C, \dots, H are infinite submatrices, and \mathbf{a}, \mathbf{b} , and \mathbf{c} are vectors which constitute the expansion coefficients of the eigenfunctions of μ_d, u_d , and v_d , respectively. The expressions for elements of submatrices A, B, C, \dots, H and an algorithm for evaluating them are given in the Appendix.

The eigenvalue problem is solved numerically by truncating the infinite matrix to a 150×150 matrix. The accuracy of eigenvalues is evaluated by comparing their values with those obtained from a smaller matrix, usually of size 135×135 .

The complex eigenvalues corresponding to global unstable modes can be obtained generally accurately if $|\hat{\omega}_i| > 0.1$, where $\hat{\omega}_i$ is the imaginary part of $\hat{\omega}$, and we will discuss the stability of equilibrium models of NGC 3115 constructed in § II.

IV. RESULTS AND DISCUSSIONS

Oscillation spectra of bisymmetric perturbations ($m = 2$) of a number of models ($s = 0, 0.1, 0.2, 0.25, 0.28$, and 0.3) along a sequence are examined using the formulation described in § III. The haloless ($s = 0$) model has a number of unstable growing modes which are of trailing spiral or barlike forms. The growth rate of the most rapidly growing global mode, $\hat{\omega}_{i\max}$, is shown for each model in Table 1. The quantity $\Delta(\hat{\omega}_{i\max})$ in Table 1 is defined by

$$\Delta(\hat{\omega}_{i\max}) = \frac{(\hat{\omega}_{i\max})_{50} - (\hat{\omega}_{i\max})_{45}}{(\hat{\omega}_{i\max})_{50}}, \quad (4.1)$$

where the subscripts 50 and 45 denote the results of calculations of the 150×150 matrix and the 135×135 matrix, respectively. It is shown that the growth rate decreases as the halo-mass fraction s increases.

A preliminary report of this work was given in Iye *et al.* (1982), but a subsequent study shows revision of Figure 3 of Iye *et al.* (1982) as in the data shown in Table 1.

The model of $s = 0.28$ still has a well-determined unstable mode with $\hat{\omega}_{i\max} = 0.09$, which corresponds to an e -folding time of 2×10^7 years. The practical requirement of stability is such that the most unstable mode of the disk of NGC 3115 should not evolve into an oscillation of significant amplitude within the age of the galaxy (10^{10} years). The model of $s = 0.28$ is, therefore, still too unstable and is not consistent with the apparent lack of any non-axisymmetric structure in NGC 3115. On the other hand the next model ($s = 0.3$) does not allow the confirmation of existence of any unstable modes with a tolerable accuracy.

It would therefore be safe to state that a halo component of

at least 30% of the total mass is required for NGC 3115 to make its disk component dynamically stable, so as to be consistent with its morphological appearance. This is admittedly a rather loose lower limit of halo mass fraction when compared with the photometric evaluation by Tsikoudi (1979), who decomposed the B -luminosity distribution into bulge and disk components and found the bulge luminosity fraction to be 84% of the total luminosity. It is important, however, to remember that this dynamical estimate with the morphology of the disk is independent of the photometric estimate and also of another dynamical estimate, for example, the virial estimate, which does not take the dynamical stability into account but just considers the equilibrium. With the improvement of theoretical codes there is room to improve our dynamical estimate to give a more strict and useful lower limit.

Our analysis is limited in several respects. First of all, we have assumed that the halo component has the same scale length as the disk component. It is likely that the halo has a larger scale length than the disk and extends farther out. Such an extended halo will stabilize the disk less efficiently, and one needs a more massive halo. This relaxation of an assumption, therefore, does not change the lower limit of s obtained in the present analysis. Next, the possibility of the overestimation of $\sigma(r)$ must be considered. The projection of the rotational velocities may contribute to the observed $\sigma(r)$ because NGC 3115 is edge-on. If the real $\sigma(r)$ is smaller, the disk becomes more unstable. Larger values of s are necessary to stabilize the disks when the models with smaller $\sigma(r)$ are examined. So, even if the overestimation of $\sigma(r)$ is real, it does not change the lower limit of s either. Another assumption, which might be of more influence, is the value of the polytropic exponent Γ . We have so far no physical ground to specify the value of Γ , although it should be in the range $1 \leq \Gamma \leq 3$ if we make use of the relation between the two-dimensional Γ and the three-dimensional γ , which is in the range $1 \leq \gamma \leq \infty$ (cf. Hunter 1972). We did not make an extensive study of the effect of Γ in this paper; such a study is a straightforward extension. Analysis is limited to $m = 2$ modes. Studying $m \neq 2$ modes may improve our estimate of the lower limit.

An analysis, similar to that in this paper, for spiral galaxies will be interesting when reliable velocity dispersion curves become available. By constructing models that are consistent with the observed kinematical data and that reproduce the observed spiral patterns as their most rapidly growing modes, one can examine the structure of disks of spiral galaxies. This *seismological* study, so to speak, may prove to be successful in improving our understanding of the structure of galaxies.

In conclusion, we have shown that (1) the modal analysis is useful for a diagnosis of structure of galaxies when reliable kinematical data, e.g., rotation curves and velocity dispersion curves, are combined with morphological data of spatial eigenfunctions of their dominant modes, and (2) application of this method to NGC 3115 results in a loose but consistent lower limit for the halo mass fraction of 30% of the total mass.

We wish to thank Dr. F. Takahara for helpful discussions, and we also thank Dr. M. Hamabe for his useful comments.

TABLE 1
GROWTH RATE OF THE MOST UNSTABLE GLOBAL MODE OF EACH MODEL

| | $s = 0.00$ | $s = 0.10$ | $s = 0.20$ | $s = 0.25$ | $s = 0.28$ | $s = 0.30$ |
|--|------------|------------|------------|------------|------------|------------|
| $\hat{\omega}_{i\max}$ | 0.656 | 0.367 | 0.177 | 0.111 | 0.094 | ... |
| $ \Delta(\hat{\omega}_{i\max}) $ | 2(-5) | 1(-4) | 4(-3) | 1(-2) | 4(-3) | ... |

APPENDIX

The (l, n) -elements of matrices A, B, \dots , and H in equation (3.2) are expressed as

$$A_{ln} = m \int_{-1}^1 \hat{P}_l^m \hat{\Omega} \hat{P}_n^m d\xi, \quad (A1)$$

$$B_{ln} = 4 \int_{-1}^1 \hat{P}_l^m \left(\frac{1-\xi}{2} \right)^{1/2} \frac{d}{d\xi} \left[\hat{\mu}_d \left(\frac{1-\xi}{2} \right)^{-1/4} \hat{P}_n^m \right] d\xi, \quad (A2)$$

$$C_{ln} = m \int_{-1}^1 \hat{P}_l^m \hat{\mu}_d \left(\frac{1-\xi}{2} \right)^{-3/4} \left(\frac{1-\xi}{2} \right)^{-1} \hat{P}_n^m d\xi, \quad (A3)$$

$$D_{ln} = 4 \int_{-1}^1 \hat{P}_l^m \left(\frac{1-\xi}{2} \right)^{5/4} \left(\frac{1+\xi}{2} \right) \frac{d}{d\xi} \left\{ \left[\frac{1}{2n+1} \left(\frac{1-\xi}{2} \right)^{1/2} - K_d \Gamma \hat{\mu}_d^{\Gamma-2} \left(\frac{1-\xi}{2} \right)^{3/2} \right] \hat{P}_n^m \right\} d\xi, \quad (A4)$$

$$F_{ln} = 2 \int_{-1}^1 \hat{P}_l^m \hat{\Omega} \hat{P}_n^m d\xi, \quad (A5)$$

$$G_{ln} = -m \int_{-1}^1 \hat{P}_l^m \left(\frac{1-\xi}{2} \right)^{3/4} \left[\frac{1}{2n+1} - K_d \Gamma \hat{\mu}_d^{\Gamma-2} \left(\frac{1-\xi}{2} \right) \right] \hat{P}_n^m d\xi, \quad (A6)$$

$$H_{ln} = \int_{-1}^1 \hat{P}_l^m \left(\frac{\hat{\kappa}^2}{2\hat{\Omega}} \right) \hat{P}_n^m d\xi. \quad (A7)$$

Since $\hat{\Omega}$ and $\hat{\kappa}^2/2\hat{\Omega}$ are independent of s , and $\hat{\mu}_d$ is proportional to $1-s$, A, F , and H are independent of s , and B and C are proportional to $1-s$. For $\Gamma = 4/3$ disks, D and G are proportional to $[1/(2n+1) - \epsilon(s)/3]$.

The first rows ($n = m$) of each matrix should be evaluated by numerical integrations, but the other elements ($n > m$) can be obtained by the recurrence formulae given in Appendix 1 of ANI. The calculating accuracy of the matrix elements is proved to be sufficiently high by examining the symmetry of each submatrix.

REFERENCES

- Ambastha, A., and Varma, R. K. 1982, *J. Ap. Astr.*, **3**, 125.
 ———, 1983, *Ap. J.*, **264**, 413.
 Aoki, S. 1984, *Astr. Ap.*, submitted.
 Aoki, S., Noguchi, M., and Iye, M. 1979, *Pub. Astr. Soc. Japan*, **31**, 737 (ANI).
 Bardeen, J. 1975, in *IAU Symposium 69, Dynamics of Stellar Systems*, ed. A. Hayli (Dordrecht: Reidel), p. 297.
 Hamabe, M. 1982, *Pub. Astr. Soc. Japan*, **34**, 423.
 Hunter, C. 1963, *M.N.R.A.S.*, **126**, 299.
 ———, 1965, *M.N.R.A.S.*, **129**, 321.
 ———, 1972, *Ann. Rev. Fluid Mech.*, **4**, 219.
 ———, 1979, *Ap. J.*, **227**, 73.
 Illingworth, G. 1981, in *Structure and Evolution of Normal Galaxies*, ed. S. M. Fall and D. Lynden-Bell (Cambridge: Cambridge University Press), p. 27.
 Illingworth, G., and Schechter, P. L. 1982, *Ap. J.*, **256**, 481 (IS).
 Iye, M. 1978, *Pub. Astr. Soc. Japan*, **30**, 223.
 Iye, M., Ueda, T., Noguchi, M., and Aoki, S. 1982, in *IAU Symposium 100, Internal Kinematics and Dynamics of Galaxies*, ed. E. Athanassoula (Dordrecht: Reidel), p. 125.
 Kuz'min, G. G. 1956, *Astr. Zh.*, **33**, 27.
 Lin, C. C., and Shu, F. H. 1964, *Ap. J.*, **140**, 646.
 Plummer, H. C. 1911, *M.N.R.A.S.*, **71**, 460.
 Rubin, V. C., Peterson, C. J., and Ford, W. K., Jr. 1980, *Ap. J.*, **239**, 50.
 Strom, K. M., Strom, S. E., Jensen, E. B., Moller, J., Thompson, L. A., and Thuan, T. X. 1977, *Ap. J.*, **212**, 335.
 Takahara, F. 1976, *Progr. Theor. Phys.*, **56**, 1665.
 ———, 1978, *Pub. Astr. Soc. Japan*, **30**, 253.
 Toomre, A. 1963, *Ap. J.*, **138**, 385.
 Tsikoudi, V. 1979, *Ap. J.*, **234**, 842.
 Yabushita, S. 1969, *M.N.R.A.S.*, **143**, 231.

S. AOKI, M. IYE, and M. NOGUCHI: Tokyo Astronomical Observatory, University of Tokyo, Mitaka, Tokyo 181, Japan

T. UEDA: Department of Astronomy, University of Tokyo, Bunkyo-ku, Tokyo 113, Japan